J Mater Sci: Mater Med (2011) 22:1383–1391
DOI 10.1007/s10856-011-4312-9

Characterization of surface modification on self-assembled monolayer-based piezoelectric crystal immunosensor for the quantification of serum α-fetoprotein

Yu-Chang Tyan · Ming-Hui Yang · Tze-Wen Chung · Wen-Cheng Chen · Ming-Chen Wang · Yi-Ling Chen · Shu-Ling Huang · Ying-Fong Huang · Shiang-Bin Jong

Received: 2 August 2010 / Accepted: 30 March 2011 / Published online: 9 April 2011

Abstract Self-assembled monolayers (SAMs) on coinage metallic material can provide versatile modeling systems for studies of interfacial electron transfer, biological interactions, molecular recognition and other interfacial phenomena. Recently, a bio-sensing system has been produced by analysis of the attachment of antibody using alkanethiols, to form SAMs on the face of Au-quartz crystal microbalance (QCM) surfaces. In this study, the attachment of anti-α-fetoprotein monoclonal antibody to a SAMs surface of 11-mercaptoundecanoic acid was achieved using water-soluble *N*-ethyl-*N*′-(3-dimethylaminopropyl) carbodiimide hydrochloride and *N*-hydroxysuccinimide as coupling agents. Surface analyses were utilized by X-ray photoelectron spectroscopy and atomic force microscopy. The quantization of immobilized antibody was characterized by the frequency shift of QCM and the radioactivity change of ^{125}I labeled antibody. The limit of detection and linear range of the calibration curve of the QCM method were 15 ng/ml and 15–850 ng/ml. The correlation coefficients of α-fetoprotein concentration between QCM and radioimmunoassay were 0.9903 and 0.9750 for the standards and serum samples, respectively. This report illustrates an investigation of SAMs for the preparation of covalently immobilized antibody biosensors.

1 Introduction

α-Fetoprotein (AFP) is a large serum glycoprotein belonging to the intriguing class of onco-developmental proteins. It is a major protein in embryonic plasma and is produced by the yolk sack, gastrointestinal tissue and fetal liver [1]. α-Fetoprotein is also a carrier protein. Its binding

Ming-Hui Yang and Ying-Fong Huang contributed equally to this work as co-first authors.

Y.-C. Tyan (✉) · S.-L. Huang · Y.-F. Huang · S.-B. Jong (✉)
Department of Medical Imaging and Radiological Sciences, Kaohsiung Medical University, 100, Shi-Chuan 1st Rd, Kaohsiung 807, Taiwan
e-mail: yctyan@kmu.edu.tw

S.-B. Jong
e-mail: jongsb@kmu.edu.tw

Y.-C. Tyan
National Sun Yat-Sen University-Kaohsiung Medical University Joint Research Center, Kaohsiung, Taiwan

Y.-C. Tyan
Center for Resources, Research and Development, Kaohsiung Medical University, Kaohsiung, Taiwan

M.-H. Yang · T.-W. Chung
Department of Chemical and Material Engineering, National Yulin University of Science and Technology, Douliou, Taiwan

W.-C. Chen
Department of Fiber and Composite Materials, Feng Chia University, Taichung, Taiwan

M.-C. Wang
Department of Biomedical Engineering, Chung Yuan Christian University, Chungli, Taiwan

Y.-L. Chen · Y.-F. Huang · S.-B. Jong
Department of Nuclear Medicine, Kaohsiung Medical University Chung-Ho Memorial Hospital, Kaohsiung, Taiwan

ligands include steroids, bilirubin, fatty acids, retinoids, and flavonoids [2]. The normal range of AFP concentration in serum is typically under 20 ng/ml and is elevated slightly for pregnant women. Moderate elevations of AFP concentration (up to 500 ng/ml) can be found in patients with chronic hepatitis [3, 4]. Moreover, patients with various liver diseases can have mild or moderate elevations of AFP expression. α-Fetoprotein has growth inhibitory and apoptotic effects on several human tumor cell-lines [5, 6]. In addition, peptides derived from AFP can suppress tumor growth [7, 8]. Its growth inhibitory effects may function individually or synergistically with growth factors [5, 9–11]. Therefore, it could indicate a pathological process and be treated as a tumor maker. The concentration of AFP is also measured during pregnancy, using maternal blood or amniotic fluid, as a screening test for subset developmental abnormalities; the concentrations principally increase in open neural tube defects and omphalocele, and decrease in Down's syndrome [12].

The conventional methods for the quantification of AFP are radioimmunoassay (RIA) and enzyme-linked immunosorbent assay (ELISA). Due to high sensitivity and specificity, both techniques have been broadly used in research and clinical fields since 1960 [13]. However, those techniques require special disposal (for RIA), high cost, and stability problems (for ELISA). Also, these methods rely on the detection of labeled molecules and are laborious and time consuming [14].

Self-assembled monolayers (SAMs) have received a great deal of attention for their fascinating potential technical applications such as nonlinear optics and device patterning [15–17]. They also have been used as an ideal model to investigate the effects of intermolecular interactions in the molecular assembly systems [18–21]. Self-assembled monolayers have been traditionally prepared by immersing a substrate into a solution containing a ligand that is reactive to the substrate surface or by exposing the substrate to the vapor of the reactive species. The most common utilization of the SAMs system is the application of alkanethiolates (AT) on gold (Au), rather than other metals such as platinum, copper, or silver, because gold does not have stable oxide compounds and easily forms a bond with sulfur. The AT SAMs not only provides an excellent model system to study fundamental aspects of surface properties such as wetting [22] and tribology [23], but also is a promising candidate for potential applications in the fields of biosensors [24], biomimetics [25] and corrosion inhibition [26].

The quartz crystal microbalance (QCM) with an A-T cut quartz slide equipped with electrodes has been used in various fields, such as environmental protection, chemical technology, medicine, food analysis, and biotechnology [27–32]. It has been widely used for substance measurement in liquid environments. Previously, research has revealed that measurements in liquid environments are very complicated. Several variations in liquid environments, such as characteristics of crystals and factors of surface interactions, should be controlled and calibrated with accurate and precise machines and mathematical formulas [33–36]. Besides, the amount of sample used in aqueous environments often requires more than can be acquired for analysis from the human body and may be a limitation for use as a clinical immunosensor. The detection theory for QCM can be explained by the Sauerbrey equation (Eq. 1), which calculates that the mass change is proportional to the oscillation frequency shift of the piezoelectric quartz crystal [37].

$$\Delta F = -2.3 \times 10^{-6} \frac{F^2 \Delta M}{A} \quad (1)$$

Equation 1: Sauerbrey equation in gas phase. ΔF: the frequency shift (Hz); F: basic oscillation frequency of piezoelectric quartz (Hz); A: the active area of QCM (cm^2); ΔM: the mass change on QCM (g).

This experiment completes a study for a potential biomedical application of functionalized SAMs with the immobilized anti-AFP monoclonal antibody, and a QCM system using the SAMs chip for AFP quantification. This type of surface is successfully used to develop a feasible procedure for producing surface-based biochips. We present the AFP concentration measured by SAMs-QCM chip and have compared the QCM data with the RIA method in serum.

2 Material and method

2.1 Atomic force microscopy image of QCM ship surface

The QCM chip (coated Au, 10 MHz, diameter of quartz: 0.8 cm, diameter of Au: 0.38 cm, Taitien, Taiwan) surface was analyzed by the atomic force microscopy (AFM). The AFM image was acquired with a Slover PRO (NT-MDT, Russia) AFM in ambient pressure. The semi-contact mode was used with a frequency of 0.5 μm/s to scan an area of 10 × 10 μm^2. The AFM probe was a golden silicon probe (NSG11, NT-MDT, Russia) with the length, width, thickness, resonant frequency and force constant as 100 mm, 35 μm, 2.0 μm, 255 kHz and 11.5 N/m^2, respectively.

2.2 Formation of SAMs on QCM chips

Quartz crystal microbalance chips were cleaned by the soxhlet extraction process using a solution (methanol and acetone 1:1) for 24 h. Then, the QCM chips were cleaned with ultra pure ethanol (RDH 32205, Riedel-deHaën).

The QCM chips were immersed into a 0.5 mM 11-mercaptoundecanoic acid (11-MUA, $C_{11}H_{22}O_2S$, 450561, Aldrich) ethanol solution for 8 h and rinsed with pure ethanol twice. The alkanethiols adsorbed spontaneously from solution onto the Au surface. The functionalized thiol groups were chemisorbed onto the Au surface via the formation of thiolate bonds. After being dried by nitrogen, the surface analysis was performed by X-ray photoelectric spectroscopy (XPS).

2.3 X-ray photoelectron spectroscopy measurement

X-ray photoelectric spectroscopy spectra were acquired with a Physical Electronics PHI 1600 ESCA photoelectron spectrometer with a magnesium anode at 400 W and 15 kV–27 mA (Mg Kα 1253.6 eV, type 10-360 hemispherical analyzer). The specimens were analyzed at an electron take-off angle of 70°, measured with respect to the surface plane. The operating conditions were as follows: pass energy 23.4 eV, base pressure in the chamber below 2×10^{-8} Pa, step size 0.05, total scan number 20, scan range 10 eV (for multiplex scan). The peaks were quantified from high-resolution spectra using a monochromatic Mg X-ray source. Elemental compositions at the surface using C 1s, O 1s and S 2p core-level spectra were measured and calculated from XPS peak areas with correction algorithms for atomic sensitivity. The XPS spectra were fitted using Voigt peak profiles and a Shirley background.

2.4 Immobilization of ^{125}I anti-AFP monoclonal antibody onto SAMs

In order to immobilize ^{125}I anti-AFP monoclonal antibody, the 11-MUA/Au surface was immersed in the solution containing coupling agents: 75 mM *N*-ethyl-*N*′-(3-dimethylaminopropyl) carbodiimide hydrochloride (EDC, E-6383, Sigma) and 15 mM *N*-hydroxysuccinimide (NHS, H-7377, Sigma) at 4°C for 30 min [38, 39]. Water-soluble EDC and NHS were used to activate O=C–OH [40, 41] and then the EDC-NHS solution was replaced by a phosphate buffer saline (PBS, URPBS001, UniRegion Bio-Tech), containing 0.2 μg/ml AFP-antibody (Cisbio Bioassays) at 4°C for 24 h. The SAMs chips were thereafter washed by D.I. water and freeze-dried. During the reactions, EDC converted the carboxylic acid group into a reactive intermediate, which was attacked by amines. Figure 1 shows the experimental design and the SAMs structure with immobilized ^{125}I anti-AFP monoclonal antibody. The radioactivity of each ^{125}I anti-AFP monoclonal antibody immobilized QCM chip was measured by the Scaler cobra II series auto-gamma counting system (Packard, USA, Energy window: 15–75 keV, detection efficiency > 75%, resolution < 34%, detector background < 25 cpm).

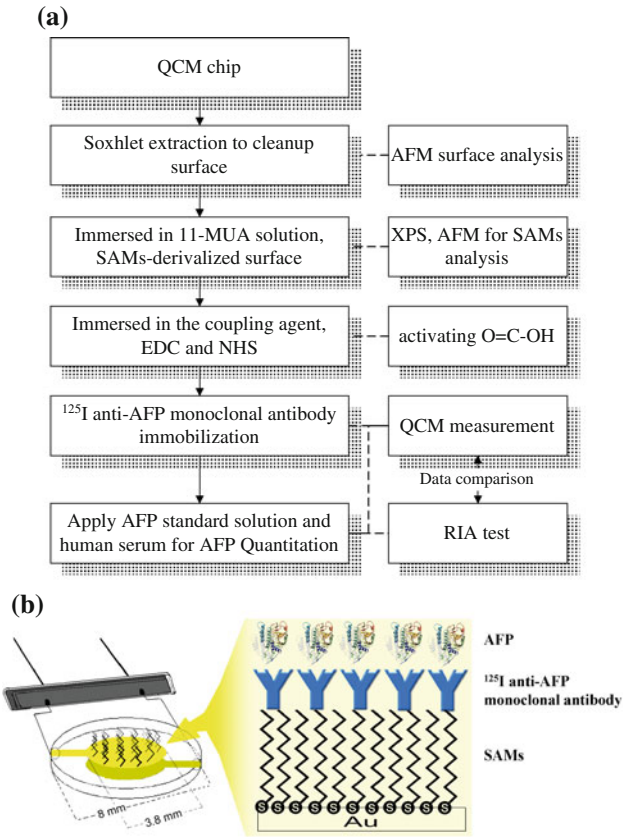

Fig. 1 **a** The scheme of the overall experiment to quantify the AFP concentration by a SAMs-QCM system. **b** The structure of SAMs formation and ^{125}I anti-AFP monoclonal antibody immobilization onto SAMs

2.5 QCM frequency measurement

The frequency shift of QCM chips was measured by a muti-channel piezoelectric frequency counter with computer signal analysis software (PZ-1001 Immuno-Biosensor System, Universal Sensors Inc., Metairie, LA, USA). For the AFP standard curve and LOD of QCM frequency measurements, the standard solutions with difference concentrations were prepared by dissolving AFP in normal saline and ranged from 5 to 1000 ng/ml. On the other hand, serum specimens were spiked with highly purified human AFP into fetal calf serum in different concentrations (30–400 ng/ml) to simulate unknown samples for QCM and RIA tests (AFP, F8004, Sigma; fetal calf serum, 16170-078, Invitrogen).

In the QCM frequency measurement of AFP, 10 μl of the AFP standard solutions or serum samples were deposited on the anti-AFP monoclonal antibody immobilized chip. The chips were agitated slowly at room temperature for 10 min, rinsed by D.I. water, and then air-dried. The QCM instrument was operated in a humidity-controlled cabinet and the humidity was under 50% RH to prevent the moisture interference. Each concentration was examined

six times per chip in a total of six chips. The same procedures were used for the measurement of serum samples.

2.6 Radioimmunoassay of AFP

The AFP concentrations were measured by alpha-fetoprotein ELSA kits (ELSA2-AFP, Cisbio Bioassays). The AFP standards (from the ELSA kit) or AFP spiked serum samples (as above) were sandwiched between anti-AFP monoclonal antibody coated on the tube and ^{125}I labeled anti-AFP. All standards and serum samples were counted in duplicate by the Scaler cobra II series auto-gamma counting system. The detection limit of this assay in AFP concentrations was 0.5 ng/ml.

3 Results and discussion

The immobilization methods of antibodies in optimal conditions through physical passive adsorption, protein binding, and covalence binding have been compared in previous studies [42–44]. Misleading results have been noted using various biomolecule adsorptions, such as physical passive adsorption and protein binding methods (as for protein A) [45–47]. Therefore, a SAMs surface offers a suitable intermolecular interaction surface for biomolecule immobilization. The functional terminal group and the length of the alkyl chain of SAMs affect the efficiency of immobilization. Previous studies have shown that the unsymmetrical dialkane sulfide monolayer and the short carboxylate chain of disulfide and thiol each had less dense and ordered structure compared with alkanethoil monolayers [48–51]. Hence, 11-MUA was utilized in this study, and its existence on the QCM chips was proven through XPS.

4 Surface characterization

A rough chip exterior may cause an uneven SAMs surface. To investigate the topology characteristics of the surface, AFM was used to observe the QCM chip surface. In Fig. 2, the image of the topographical map taken in the semi-contact mode of a 10 × 10 μm^2 zone is shown. Figure 2a is a surface image of the QCM chip, and Fig. 2b shows the three-dimensional structure. This impressive image in Fig. 2b shows a very clear set of surface roughness with a mean depth about 1.2 μm. A rough surface may provide the opportunity to increase the reaction surface and the effectiveness antibody immobilization. Most SAMs studies were established on the ideal, well-ordered and smooth single-crystal silicon (100 or 111) wafers primed with a metal adhesion layer [52, 53]. On the single-crystal silicon wafers, theoretically, all alkanethiols should be bound onto the SAMs surface as an Au–S–C– structure. Unlike the surface of ideal single-crystal silicon wafers, the rough QCM chip surface may be composed of three types of SAMs structures: alkanethiol bound, attachment by adhesion, and sulfonite-Au bonding. The XPS (S 2p, dialkylsulfide and sulfonite species) indicated that the SAMs deposited onto the QCM surface was non-regular.

The binding structure of the SAMs on the metal surface was monitored by XPS. In the XPS measurements, the variations of O 1s and S 2p with respect to C 1 s signal ratios were correlated with the significant presence of chemical species at the SAMs surfaces. The C 1s, O 1s, and S 2p spectra showed the existence of 11-MUA onto the gold-coated QCM chips. The XPS spectra of 11-MUA onto the gold electrode are shown in Fig. 3.

In the XPS C 1s spectrum, the peaks of binding energies of core levels at 285.0, 286.9, and 288.8 eV were assigned to the –C–C–, –C–S–, and O=C–O structures, respectively. The C 1s core-level spectrum of the peak at 286.9 eV and the S 2p spectrum of the peak in 162.0 eV confirmed the Au–S–$(CH_2)_n^-$ existence. The C 1s core-level spectrum of the peak at 288.8 eV and the O 1s spectrum of the peaks at 532.0 and 533.2 eV provided evidence that the terminal groups of SAMs on the QCM chips were the carboxylic acid groups.

In the O 1s spectrum, the peaks of binding energies of O 1s core levels at 532.0 and 533.2 eV were assigned to the carboxylic acid group (O*=C–O and O=C–O* for the * marked O, respectively) structure, which was the characteristic group of 11-MUA.

In the S 2p spectrum, the peaks of binding energies of core levels at 162.0, 163.2, and 169.30 eV were assigned to the Au–S–C–, dialkylsulfide, and SO_3^-, respectively. The S 2p spectrum inculcated a doublet structure due to the presence of the S $2p_{3/2}$ and S $2p_{1/2}$ peaks using a 2:1 peak area ratio with a 1.2 eV splitting as shown in Fig. 3. The peak at 162.0 eV was assigned to sulfur atoms bound to the gold surface as a thiolate species [54]. The S 2p spectrum of peak at 163.2 eV was assigned to dialkylsulfide as unbound thiol, which may be due to alkanethiols physisorbed as a double layer or adhesion of alkanethiols [50]. The S 2p spectrum of peak at 168.5 eV can be attributed to a sulfonite species (SO_3^-). The sulfonite species formation was from the rapid oxidation of sulfur on the 11-MUA modified QCM chip surface. Since the sulfur atom was at the bottom of the 11-MUA chains, the XPS signal in detecting S–O was much weaker then that of C with O, which was on the top of the chain. Thus, it was not feasible to fit the S–O peak in the O 1s spectrum. Although the SAMs structure on the QCM chip was not ideal, it did not affect the antibody immobilization onto the tail group because the EDC and NHS only functioned on the carboxylic acid group.

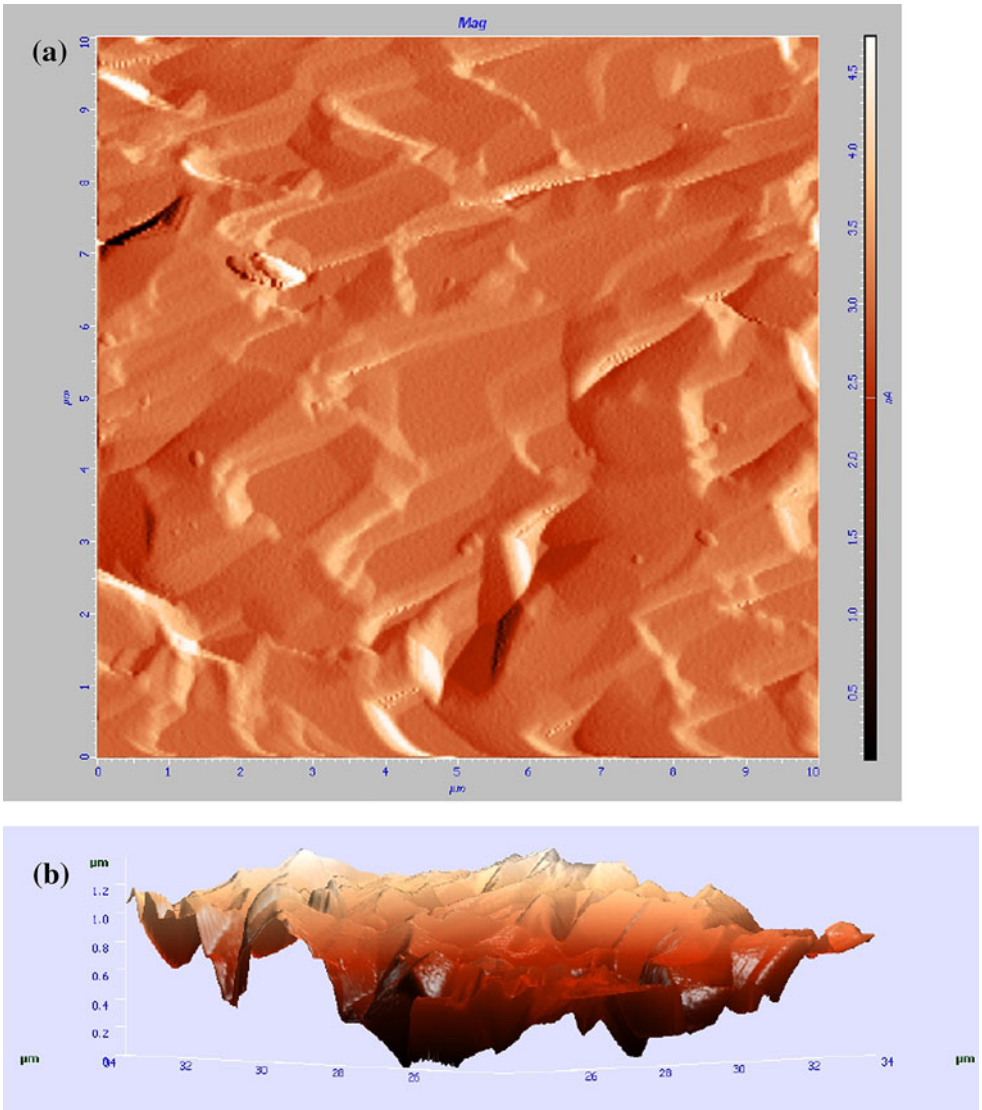

Fig. 2 AFM images of the Au-covered QCM chip. **a** Blank, 10 × 10 μm, **b** blank, 3D structure. AFM measurements could also be used for measuring the surface roughness of the QCM chip. The mean surface roughness was 1.2 nm

Antibody immobilization on SAMs proceeds via a two-step immobilization mechanism: a rapid preliminary physical adsorption, and then the covalent attachment between amino groups of the antibody by coupling agents [55]. The key benefit derived from longer chains was that the coverage of the substrate could be achieved with fewer chains. Antibodies are bulky macromolecules and longer alkyl chains can separate antibodies in space and thus increase the efficiency to immobilize more antibodies [56]. Thus, it may also increase the possibility of physical adsorption, where in situ washing can also be used to remove the physical adsorptions efficiently.

4.1 ^{125}I anti-AFP monoclonal antibody immobilized Surfaces

The QCM frequency variation after SAMs formation was lowered to around -12.7 ± 1.1 Hz (Fig. 4). In this experiment, water-soluble EDC and NHS were used to convert the carboxylic acid of the 11-MUA monolayer to a NHS ester. This reaction activated the 11-MUA-NHS ester monolayer with an aqueous solution of an amine or ammonia which formed an amide bond with the surface. For the QCM and RIA measurements, the frequency variations and count rates were correlated with the data from ^{125}I anti-AFP monoclonal antibody immobilized SAMs-QCM surface. The QCM frequency decreased after the immobilization of ^{125}I anti-AFP monoclonal antibody (Fig. 4). Its average and the coefficient of variations were -216.8 ± 41.9 Hz. The count rate of the RIA of ^{125}I anti-AFP monoclonal antibody was 139 ± 16.9 cpm (counts per minute). Thus, the poly-complex between ^{125}I anti-AFP monoclonal antibody and 11-MUA was formed; amino groups in ^{125}I anti-AFP monoclonal antibodies formed complexes with carboxyl groups of 11-MUA. In the QCM measurements, the variations of QCM frequency shift were correlated with the

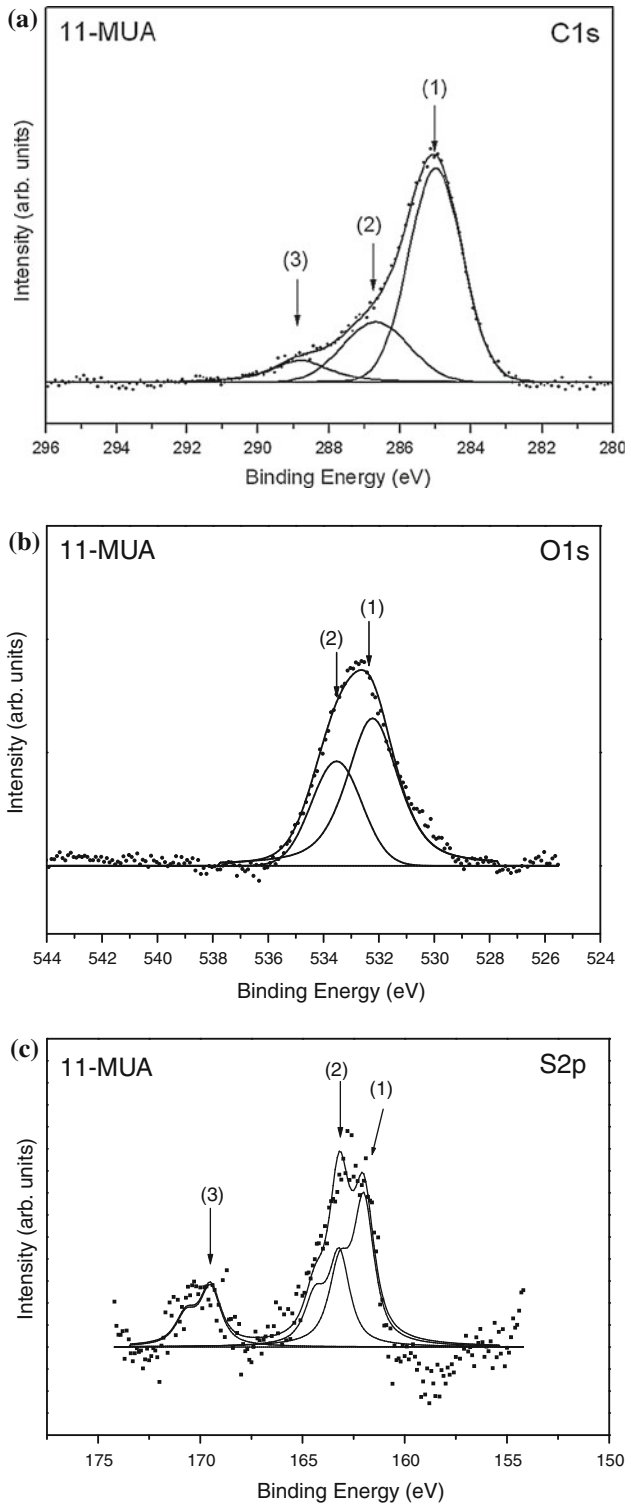

Fig. 3 XPS spectra of the 11-MUA modified SAMs surface. **a** C 1s, the binding energy at (*1*) 285.0 eV, (*2*) 286.9 eV, and (*3*) 288.8 eV were assigned to the –C–C–, –C–S–, and O=C–O, **b** O 1s, the binding energy at (*1*) 532.0 eV and (*2*) 533.2 eV were assigned to the carboxylic acid group, **c** S 2p, the binding energy at (*1*) 162.0 eV, (*2*) 163.2 eV, and (*3*) 169.30 eV were assigned to the Au–S–C–, dialkylsulfide, and SO_3^-, respectively

changes of count rates of the RIA on the ^{125}I anti-AFP monoclonal antibody immobilized QCM surface. The amount of the ^{125}I anti-AFP monoclonal antibody immobilized onto QCM chips was 44.02 ± 0.49 ng/cm^2. In this study, the surface modification of QCM was analyzed, and the formation of SAMs structure and antibody adsorption were also confirmed.

4.2 Quantitation of AFP

Immunosensors, having the specificity of antibody–antigen (Ab–Ag) affinities and the high sensitivities of various physical transducers, have gained attention for clinical diagnosis [57]. This study combined both techniques of SAMs and QCM, where a decrease of the resonance frequency is correlated with the mass accumulated on its surface. Moisture control of the antibody immobilized onto QCM chips in this experiment is used through the freeze-drying method. As compared with other drying methods, freeze-drying is capable of dehydration without deformation of biomaterial substances, such as proteins and enzymes. Considering the activity of antibody and antigen for these experiments and commercial kits, freeze-drying is utilized to sublimate moisture on the surface of QCM chips. In this study, all of the QCM measurements were in the humidity-controlled cabinet and the humidity was under 50% RH to prevent moisture interference. The preparation of chips and the tests of serum samples were done under humidity-controlled conditions because the high humidity will increase the frequency shift and bias the results.

After the SAMs formation and AFP-antibody immobilization, the QCM chips were used to measure the concentrations of AFP standard solutions and serum samples. To monitor the feasibility of the QCM method for AFP measurement, the AFP calibration curve was established by

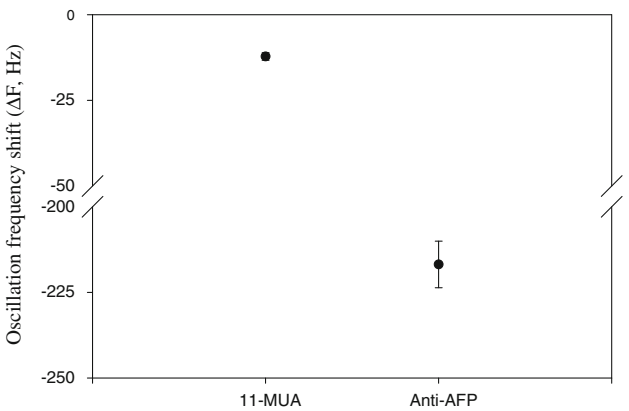

Fig. 4 The oscillation frequency shift of SAMs-QCM chips after 11-MUA and anti-AFP monoclonal antibody immobilization

utilizing the QCM chip to characterize AFP standard solutions by different concentrations from 5 to 1000 ng/ml. The frequency of the blank was used as a baseline. The frequency of the QCM chip was linearly decreased with the elevation of the AFP concentration. Thus, the amount of negative oscillation frequency shift ($-\Delta F$) was elevated.

The LOD was described as the smallest detectable amount of AFP adsorbed onto the QCM sensor. It used the peak-to-peak value of the noise range (S/N ratio) in the QCM frequency shifts. In this study, the average of S/N ratios of the QCM frequency shifts after antibody immobilization was around 1.89, which was over three times of the standard deviation of the background noise (19.97 Hz). Under these criteria, the LOD of this QCM system for AFP detection was around 15 ng/ml and the linear range of the calibration curve of the QCM method was 15–850 ng/ml.

Figure 5 shows the analytic results of the calibration curve, which was plotted with the QCM frequency shift against the actual AFP concentrations. Compared to the actual AFP concentrations, the QCM data was linearized and generated a regression equation as follows: $y = -0.2196x - 34.453$ (x-axis, AFP concentration; y-axis, frequency shift; $R^2 = 0.9903$). It corresponds to the Sauerbrey equation where the frequency shift solely depends on the mass change. In other words, compounds with larger masses will cause more frequency shift than those of smaller masses. In theory, the correlation between the difference of oscillation frequency ($-\Delta F$) and the AFP concentration should be noted as: $C_{(\mathrm{AFP})} = k\cdot(-\Delta F) + b$ and $b = 0$. However, the background noise amplitude of the blank chip also occurred. In this study, the b value in the equation was -34.453. Although the QCM chip was freeze-dried, the background noise amplitude may be due to the process of antibody immobilization through wet graft and thus increased the amplitude of oscillation of the QCM.

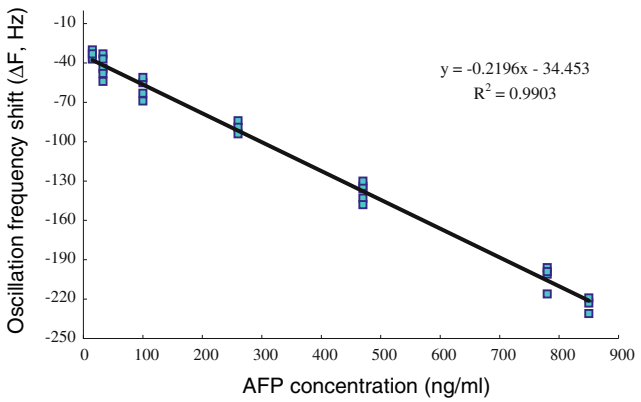

Fig. 5 The calibration curve for AFP standards using anti-α-fetoprotein monoclonal antibody immobilized QCM chips. The linearity and correlation coefficient were obtained as $y = -0.2196x - 34.453$ and $R^2 = 0.9903$

The AFP concentrations in serum samples were calculated using the interpolation of the calibration curve and RIA methods, respectively. Figure 6 shows the correlation of AFP concentrations measured by the QCM and RIA methods. In this study, different amounts of highly purified human AFP were spiked into fetal calf serum to simulate unknown samples, which were then examined by RIA and QCM methods. The linear regression equation for these data is as follows: $y = 1.0071x + 2.6747$ (x-axis, the concentration measured by RIA, y-axis, the concentrations obtained by QCM, $R^2 = 0.9750$). The variations between the results of QCM frequency shifts and RIA measurements were acceptable and comparable to theoretical concentrations. The experimental results showed an excellent correlation between RIA and QCM methods for AFP detection. The materials for SAMs-QCM are easy to obtain, and this technique is simple and easy to apply on surface-based diagnostics or biosensors. Thus, the QCM method may provide a reference method for measuring serum AFP in a laboratory and may be more feasible for clinical applications than the standard methods.

5 Conclusions

This study provides an example of the 11-MUA SAM applications of the QCM chip. self-assembled monolayer formation provides an easy technique to prepare the structure that can be further functionalized with biomolecules to yield bio-recognition surfaces for medical devices. The carboxyl functional thiol monolayer offers an excellent approach to immobilize antibodies for selected sensing of different analytes. The application of SAMs for the immobilization of antibodies onto Au surfaces has a considerable potential in application of reproducible and reliable biosensors. In this study, the quantization of immobilized antibodies was measured by the shift of QCM frequency and the radioactivity change of ^{125}I labeled

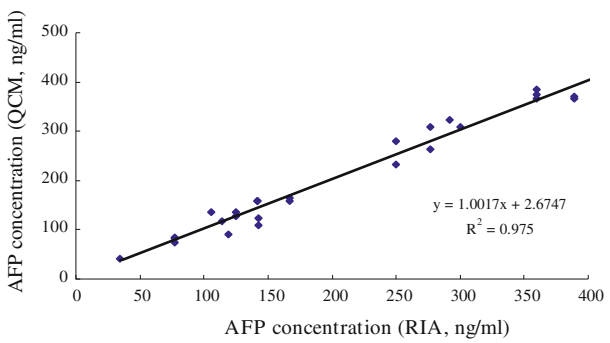

Fig. 6 Detection of APF in serum samples using QCM chips and RIA test. The correlation coefficient between the two methods was 0.9750

antibodies. The LOD of QCM was 15 ng/ml, and the linear range of the calibration curve of QCM method was 15–850 ng/ml. The correlation coefficients between QCM and RIA were 0.9903 and 0.9750 for AFP in the standards and serum samples, respectively. Compared with RIA methods, the QCM method was simple and rapid without multiple labeling and purification steps. Our system is different from the conventional approaches in that it operates in the gas phase, not the liquid phase. As a result, there is no waiting time for the frequency to reach stability. In summary, we have presented the modification of the Au interface via 11-MUA SAMs and have proved that the SAMs on Au can be a valid bio-detection chip for AFP concentration analysis by QCM. This assay design of the sensor may develop a potential reference procedure for AFP measurement and has wide applicability in the clinical setting.

Acknowledgments This work was supported by research grants, Q097004 from the Kaohsiung Medical University Research Foundation, NSC96-2321-B-037-006 and NSC97-2320-B-037-012-MY3 from the National Science Council, Taiwan, R.O.C.

References

1. Bergstrand CG, Czar B. Demonstration of a new protein fraction in serum from the human fetus. Scand J Clin Lab Invest. 1956;8:174–9.
2. Mizejewski GJ. Alpha-fetoprotein as a biologic response modifier: relevance to domain and subdomain structure. Proc Soc Exp Biol Med. 1997;215:333–62.
3. Hu KQ, Kyulo NL, Lim N, Elhazin B, Hillebrand DJ, Bock T. Clinical significance of elevated alpha-fetoprotein (AFP) in patients with chronic hepatitis C, but not hepatocellular carcinoma. Am J Gastroenterol. 2004;99:860–5.
4. Di Bisceglie AM, Hoofnagle JH. Elevations in serum alpha-fetoprotein levels in patients with chronic hepatitis B. Cancer. 1989;64:2117–20.
5. Dudich E, Semenkoval L, Gorbatova E, Dudich I, Khromykh L, Tatulov E, Grechko G, Sukhikh G. Growth-regulative activity of human alpha-fetoprotein for different types of tumor and normal cells. Tumor Biol. 1998;19:30–40.
6. Semenkova L, Dudich D, Dudich I, Tokhtamisheva N, Tatulov E, Okruzhnov Y, Garcia-Foncillas J, Palop-Cubillo JA, Korpela T. Alpha-fetoprotein positively regulates cytochrome c-mediated caspase activation and apoptosome complex formation. Eur J Biochem. 2003;270:4388–99.
7. DeFreest LA, Mesfin FB, Joseph L, McLeod DJ, Stallmer A, Reddy S, Balulad SS, Jacobson HI, Andersen TT, Bennett JA. Synthetic peptide derived from α-fetoprotein inhibits growth of human breast cancer, investigation of the pharmacophore and synthesis optimization. J Pept Res. 2004;63:409–19.
8. Andersen TT, Georgekutty J, DeFreest LA, Amaratunga G, Narendran A, Lemanski N, Jacobson HI, Bennett JA. An α-fetoprotein-derived peptide reduces the uterine hyperplasia and increases the antitumour effect of tamoxifen. Br J Cancer. 2007; 97:327–33.
9. Wang XW, Xu B. Stimulation of tumor-cell growth by alpha-fetoprotein. Int J Cancer. 1998;75:596–9.
10. Leal JA, May JV, Keel BA. Human alpha-fetoprotein enhances growth factor proliferative activity upon porcine granulosa cells in monolayer culture. Endocrinology. 1990;126:669–71.
11. Liang OD, Korff T, Eckhardt J, Rifaat J, Baal N, Herr F, Preissner KT, Zygmunt M. Oncodevelopmental alpha-fetoprotein acts as a selective proangiogenic factor on endothelial cell from the feto-maternal unit. J Clin Endocrinol Metab. 2004;89:1415–22.
12. Canick JA, Kellner LH, Bombard AT. Prenatal screening for open neural tube defects. Clin Lab Med. 2003;23:385–94.
13. Catt K, Tregear GW. Solid-phase radioimmunoassay in antibody-coated tubes. Science. 1967;158:1570–2.
14. Chou SF, Hsu WL, Hwang JM, Chen CY. Determination of alpha-fetoprotein in human serum by a quartz crystal microbalance-based immunosensor. Clin Chem. 2002;48:913–8.
15. Horne JC, Blanchard GJ. The role of substrate identity in determining monolayer motional relaxation dynamics. J Am Chem Soc. 1998;120:6336–44.
16. Morhard F, Schumacher J, Lenenbach A, Wilhelm T, Dahint R, Grunze M, Everhart DS. Optical diffraction: a new concept for rapid on-line detection of chemical and biochemical analytes. Proc Electrochem Soc. 1997;97:1058–65.
17. Bierbaum K, Grunze M, Baski AA, Chi LF, Schrepp W, Fuchs H. Growth of self-assembled *n*-alkyltrichlorosilane films on Si(100) investigated by atomic force microscopy. Langmuir. 1995;11: 2143–50.
18. Schertel A, Wöll C, Grunze M. Identification of mono- and bidentate carboxylate surface species on Cu(111) using x-ray absorption spectroscopy. J Phys IV. 1997;7:537–8.
19. Yan C, Zharnikov M, Gölzhäuser A, Grunze M. Preparation and characterization of self-assembled monolayers on indium tin oxide. Langmuir. 2000;16:6208–15.
20. Himmel HJ, Weiss K, Jäger B, Dannenberger O, Grunze M, Woell C. Ultrahigh vacuum study on the reactivity of organic surfaces terminated by –OH and –COOH groups prepared by self-assembly of functionalized alkanethiols on Au substrates. Langmuir. 1997;13:4943–7.
21. Jung C, Dannenberger O, Xu Y, Buck M, Grunze M. Self-assembled monolayers from organosulfur compounds: a comparison between sulfides, disulfides, and thiols. Langmuir. 1998; 14:1103–7.
22. Laibinis PE, Nuzzo RG, Whitesides GM. The structure of monolayers formed by coadsorption of two *n*-alkanethiols of different chain lengths on gold and its relation to wetting. J Phys Chem. 1992;96:5097–105.
23. Joyce SA, Thomas RC, Houston JE, Michalske TA, Crooks RM. Mechanical relaxation of organic monolayer films measured by force microscopy. Phys Rev Lett. 1992;68:2790–3.
24. Gooding JJ, Hibbert DB. The application of alkanethiol self assembled monolayers to enzyme electrodes. Trends Anal Chem. 1999;18:525–32.
25. Erdelen C, Haeussling L, Naumann R, Ringsdorf H, Wolf H, Yang J, Liley M, Spinke J, Knoll W. Self-assembled disulfide-functionalized amphiphilic copolymers on gold. Langmuir. 1994;10:1246–50.
26. Laibinis PE, Whitesides GM. Self-assembled monolayers of *n*-alkanethiolates on copper are barrier films that protect the metal against oxidation by air. J Am Chem Soc. 1992;114:9022–8.
27. King WH. Piezoelectric sorption detector. Anal Chem. 1964; 36:1735–9.
28. Guilbault GG. Determination of formaldehyde with an enzyme-coated piezoelectric crystal detector. Anal Chem. 1983;55: 1682–4.
29. Guilbault GG, Jordan JM, Scheide E. Analytical uses of piezoelectric crystals. Crit Rev Anal Chem. 1988;19:1–28.
30. Guilbault GG, Luong JH. Gas phase biosensors. J Biotechnol. 1988;9:1–9.

31. Guilbault GG, Hock B, Schmid RA. A piezoelectric immunobiosensor for atrazine in drinking water. Biosens Bioelectron. 1992;7:411–9.
32. Fawcett NC, Evans JA, Chen LC, Flowers N. Nucleic acid hybridization detected by piezoelectric resonance. Anal Lett. 1988;21:1099–114.
33. Attli BS, Suleman AA. A piezoelectric immunosensor for the detection of cocaine. Microchem J. 1996;54:174–9.
34. Nie LH, Zhang XT, Yao SZ. Determination of quinine in some pharmaceutical preparations using a ring-coated piezoelectric sensor. J Pharm Biomed Anal. 1992;10:529–33.
35. Muramatsu H, Tamiya E, Karube I. Computation of equivalent circuit parameters of quartz crystals in contact with liquids and study of liquid properties. Anal Chem. 1988;60:2142–6.
36. Voinova MV, Jonson M, Kasemo B. Missing mass effect in biosensor's QCM applications. Biosens Bioelectron. 2002;17:835–41.
37. O'Sullivan CK, Guilbault GG. Commercial quartz crystal microbalances: theory and applications. Biosens Bioelectron. 1999;14:663–70.
38. van Delden CJ, Lens JP, Kooyman RP, Engbers GE, Feijen J. Heparinization of gas plasma-modified polystyrene surfaces and the interactions of these surfaces with proteins studied with surface plasmon resonance. Biomaterials. 1997;18:845–52.
39. Kuijpers AJ, van Wachem PB, van Luyn MJ, Brouwer LA, Engbers GH, Krijgsveld J, Zaat SA, Dankert J, Feijen J. In vitro and in vivo evaluation of gelatin-chondroitin sulphate hydrogels for controlled release of antibacterial proteins. Biomaterials. 2000;21:1763–72.
40. Kang IK, Kwon BK, Lee JH, Lee HB. Immobilization of proteins on poly(methyl methacrylate) films. Biomaterials. 1993;14:787–92.
41. Tyan YC, Liao JD, Klauser R, Wu ID, Weng CC. Assessment and characterization of degradation effect for the varied degrees of ultra-violet radiation onto the collagen-bonded polypropylene non-woven fabric surfaces. Biomaterials. 2002;23:65–76.
42. Butler JE, Ni L, Nessler R, Joshi KS, Suter M, Rosenberg B, Chang J, Brown WR, Cantarerom LA. The physical and functional behavior of capture antibodies adsorbed on polystyrene. J Immunol Methods. 1992;150:77–90.
43. Muramatsu H, Dicks JM, Tamiya E, Karube I. Piezoelectric crystal biosensor modified with protein A for determination of immunoglobulins. Anal Chem. 1987;59:2760–3.
44. Babacan S, Pivarnik P, Letcher S, Rand AG. Evaluation of antibody immobilization methods for piezoelectric biosensor application. Biosens Bioelectron. 2000;15:615–21.
45. Lestelius M, Liedberg B, Tengvall P. In vitro plasma protein adsorption on ω-functionalized alkanethiolate self-assembled monolayers. Langmuir. 1997;13:5900–8.
46. Laibinis PE, Whitesides GM, Allara DL, Tao YT, Parikh AN, Nuzzo RG. A comparison of the structures and wetting properties of self-assembled monolayers of *n*-alkanethiols on the coinage metal surfaces, Cu, Ag, Au. J Am Chem Soc. 1991;113:7152–67.
47. Karpovich DS, Blanchard GJ. Direct measurement of the adsorption kinetics of alkanethiolate self-assembled monolayers on a microcrystalline gold surface. Langmuir. 1994;10:3315–22.
48. Chaki NK, Vijayamohanan K. Self-assembled monolayers as a tunable platform for biosensor applications. Biosens Bioelectron. 2002;17:1–12.
49. Moulder JF, Stick PE, Soble PE, Bomben KD. Handbook of X-ray photoelectron spectroscopy. New York: Eden Prairie Perkin-Elmer Co; 1995.
50. Collinson M, Bowden EF, Tarlov MJ. Voltammetry of covalently immobilized cytochrome C on self-assembled monolayer electrodes. Langmuir. 1992;8:1247–50.
51. Sahoo RR, Patnaik A. Binding of fullerene C60 to gold surface functionalized by self-assembled monolayers of 8-amino-1-octane thiol: a structure elucidation. J Colloid Interface Sci. 2003;268:43–9.
52. Weng CC, Liao JD, Wu YT, Wang MC, Klauser R, Grunze M, Zharnikov M. Modification of aliphatic self-assembled monolayers by free-radical-dominant plasma: the role of the plasma composition. Langmuir. 2004;20:10093–9.
53. Weng CC, Liao JD, Wu YT, Wang MC, Klauser R, Zharnikov M. Modification of monomolecular self-assembled films by nitrogen-oxygen plasma. J Phys Chem B. 2006;110:12523–9.
54. Castner DG, Hinds K, Grainger DW. X-ray photoelectron spectroscopy sulfur 2p study of organic thiol and disulfide interactions with gold surfaces. Langmuir. 1996;12:5083–6.
55. Jiang K, Schadler LS, Siegel RW, Zhang X, Zhang H, Terrones M. Protein immobilization on carbon nanotubes via a two-step process of diimide-activated amidation. J Mater Chem. 2004;14:37–9.
56. Pack SP, Kamisetty NK, Nonogawa M, Devarayapalli KC, Ohtani K, Yamada K, Yoshida Y, Kodaki T, Makino K. Direct immobilization of DNA oligomers onto the amine-functionalized glass surface for DNA microarray fabrication through the activation-free reaction of oxanine. Nucleic Acids Res. 2007;35:e110.
57. Morgan CL, Newman DJ, Price CP. Immunosensors: technology and opportunities in laboratory medicine. Clin Chem. 1996;42:193–209.